2D gravity modeling of shale diapirs in the northern margin of the West Alboran Basin

Modelado gravimétrico 2D de diapiros arcillosos en el margen norte de la Cuenca Oeste de Alborán

José Luis Sánchez-Roldán[1], Juan Ignacio Soto[1, 2] and Lorenzo Cascone[3]

[1] Departamento de Geodinámica, Universidad de Granada, Campus de Fuentenueva, 18071, Granada, España. sanchezroldanjl@gmail.com.
[2] Instituto Andaluz de Ciencias de la Tierra (UGR-CSIC), 18071 Granada, España. jsoto@ugr.es
[3] Geophysics Group, Repsol Exploración SA, C/ Méndez Álvaro 44, 28045 Madrid, España. lorenzo.cascone@repsol.com

ABSTRACT

Using a regional seismic profile in the northern margin of the West Alboran Basin, a 2D gravity model was made to assess the gravity response of shale structures in this basin. Time-depth conversion was accomplished taking interval velocities from sonic logs measured in the nearby Andalucía G1 well. Free Air gravity anomaly has been the gravity anomaly modeled, extracted from a regional dataset. During the 2D gravity modeling, various average densities and Moho depths were tested. The best gravimetric adjustment is obtained with a model which comprises seven layers: Plio-Pleistocene successions (2.00 g/cm³), Miocene successions (2.30 g/cm³), shale diapirs (lower Miocene) with three layers (2.05, 2.15 and 2.35 g/cm³; from top to bottom and 60% kaolinite and 40% smectite of average composition), crustal basement (2.82-2.75 g/cm³) and lithosphere mantle (3.20 g/cm³).

Key-words: *shale tectonics, gravity modeling, West Alboran Basin.*

RESUMEN

Usando un perfil sísmico regional del margen norte de la Cuenca Oeste de Alborán se ha realizado un modelo gravimétrico 2D para valorar la respuesta gravimétrica de las estructuras arcillosas en esta cuenca. Se realizó una conversión tiempo-profundidad tomando velocidades de intervalo procedentes de velocidades sónicas medidas en el pozo Andalucía G1. La anomalía modelada a lo largo de este perfil ha sido la de Aire Libre, extraída de datos regionales. Para el modelo gravimétrico 2D se han ensayado diversas densidades medias de los sedimentos y del basamento, así como la profundidad de la Moho. El mejor ajuste gravimétrico se obtiene con un modelo que comprende siete capas: sucesiones Plio-Pleistocena (2,00 g/cm³), Miocena (2,30 g/cm³), diapiros de arcilla de edad Mioceno Inferior constituidos por tres capas (2,05, 2,15 y 2,35 g/cm³; de arriba a abajo y de composición media 60% caolinita y 30% esmectita), basamento cortical (entre 2,82-2,75 g/cm³) y manto de la litosfera (3,20 g/cm³).

Palabras clave: *tectónica arcillosa, modelado gravimétrico, Cuenca Oeste de Alborán.*

Geogaceta, 62 (2017), 71-74
ISSN (versión impresa): 0213-683X
ISSN (Internet): 2173-6545

Recepción: 31 de enero de 2017
Revisión: 27 de marzo de 2017
Aceptación: 26 de abril 2017

Introduction

Studies on shale tectonics are scarce in comparison with those devoted to salt tectonics, although similar geometries can be formed by the upward movement of a weak sedimentary layer (source layer). The lower density of the source layer initially promotes deformation and flow. Nevertheless, the main difference lies on the contrasting rheology of salt compared with shales (*e.g.* Wood, 2012). Salt usually maintains a constant density/depth relation, whereas shales increase their density with depth. This variation of density in shales is controlled not only by the clay composition and transformation during burial, but also by the compaction trend and the effects of the interstitial fluids (*e.g.* Wood, 2012).

Methods of 2D gravity modeling can be used to refine the geometry of large sedimentary bodies and estimate their density. In the case of shale diapirs, variations of average composition due to different clay mineralogy can be modeled.

With this intention, a gravity model was made in the northern margin of the West Alboran Basin (WAB), where the presence of mobile shales and mud volcanoes is well known (Pérez-Belzuz *et al.*, 1997; Comas *et al.*, 1999; Talukder *et al.*, 2003; Soto *et al.*, 2010; Fig. 1).

Although mud volcanoes in the area have been sampled and analyzed, the composition of the extruded sediments, the clay-mineralogy and composition of the shale diapirs remain unknown because none of the exploration wells drilled these bodies (Jurado and Comas, 1992; Comas *et al.*, 1999).

Geological Setting

The studied area is located in the northwestern margin of the Alboran Sea Basin, behind the front of the Gibraltar Arc. Three main sub-basins have been differentiated: the West Alboran Basin (WAB), East Alboran Basin (EAB), and South Alboran Basin (SAB) (Fig. 1).

The major accumulation of sediments in the Alboran Basin occurs in the WAB, with up to 8 km of thickness (*e.g.* Soto *et al.*,

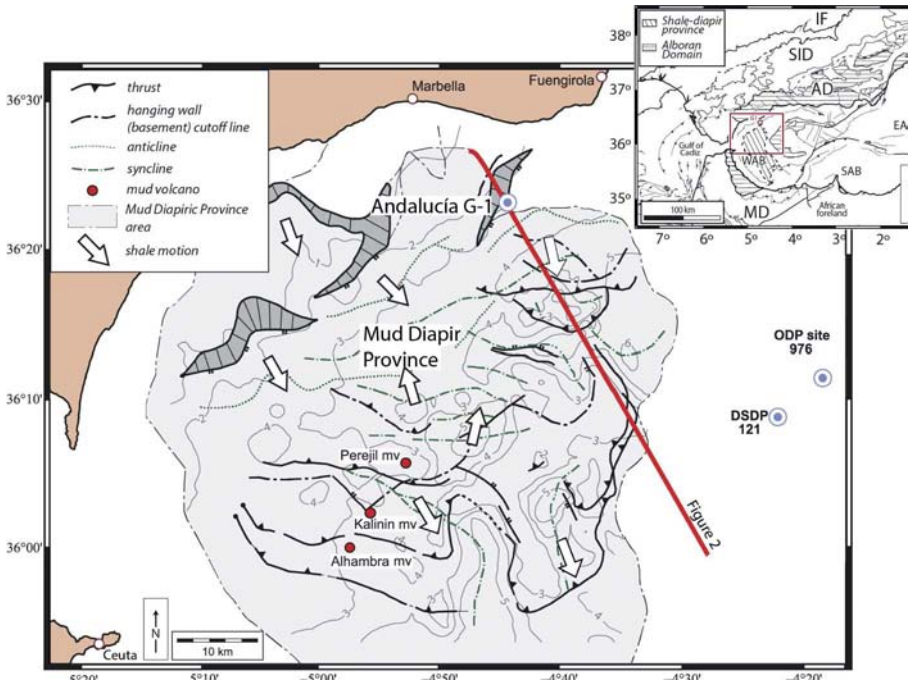

Fig. 1.- Simplified tectonic map of the mobile shale unit (Un. VI) in the northern margin of the WAB. Inset shows the geological setting of the studied area. Gray infill marks the Mud Diapir Province. Shale migration is indicated by the white arrows. Time contours (1 s twtt) for the upper boundary of Un. VI (R5 discontinuity) is also included. Taken from Soto *et al.* (2010). The modeled seismic profile shown in figure 2 is also included. AD = Alboran Domain; DSDP = Deep Sea Drilling Project; EAB = East Alboran Basin; IF = Iberian Foreland; MD = Maghrebian Domain; ODP = Ocean Drilling Project; SAB = South Alboran Basin; SID = South Iberian Domain; WAB = West Alboran Basin. See color figure in the web.

Fig. 1.- Mapa tectónico simplificado de la unidad de arcillas móviles (Un. VI) en el margen norte de la WAB. El recuadro muestra el marco geológico del área estudiada. La trama gris señala la Provincia Diapírica de Lodo en el área de estudio. La migración de esta unidad se indica con las flechas blancas. Se incluyen también las líneas de contorno (intervalo 1 s en tiempo doble) para el techo de la Un. VI (discontinuidad R5). Tomado de Soto* et al. *(2010). Se señala la posición del perfil sísmico modelado (Fig. 2). AD = Dominio de Alborán; DSDP = Deep Sea Drilling Project; EAB = Cuenca Este de Alborán; IF = Antepais de Iberia; MD = Dominio Magrebí; ODP = Ocean Drilling Project; SAB = Cuenca Sur de Alborán; SID = Dominio Sud-Ibérico; WAB = Cuenca Oeste de Alborán. Ver figura en color en la web.

2008). The sedimentary infill of the basin is classically grouped in 6 seismic-stratigraphic units (Comas *et al.*, 1999): Unit I (Pliocene-Pleistocene): mostly pelagic marls, muddy turbidites, hemipelagic clays and rare silty sand turbidites. Unit II (Messinian): marine and lacustrine sandy turbidites with fine laminated sediments and some gypsum and anhydrite levels. Unit III (Tortonian): sandstones, with claystone and silty clay beds (turbidite facies). Unit IV (Lower Tortonian-Serravallian) and Unit Va (Serravallian-Upper Langhian): graded sand-silt-clay turbidite sequences and turbiditic muds. Unit Vb (Upper Langhian) and Unit VI (Aquitanian-Burdigalian): under-compacted shales with interbedded sandy and pebble intervals.

The studied shale diapirs are sourced in Unit VI. Local information from *in-situ* sampling of mud volcanoes (formed by matrix-supported mud breccia with reworked rock clasts) provides compositional data, such as clay mineralogy or fluid content, and age. Based on the presence of lower Miocene calcareous nannofossils in the mud matrix, overpressured shales are attributed to the Aquitanian-Burdigalian (*e.g.* Sautkin *et al.*, 2003; Gennari *et al.*, 2013).

Low sonic velocity, together with low density and resistivity values are characteristic of Unit Vb and Unit VI (Jurado and Comas, 1992). Thermally induced overpressures seem to occur within Unit VI, according to temperature estimate and logging modeling (Fernández-Ibáñez and Soto, 2017).

Shale Diapirism in WAB

Diapirism in the West Alboran Basin has been documented by many authors (*e.g.*, Pérez-Belzuz *et al.*, 1997; Comas *et al.*, 1999; Talukder *et al.*, 2003; Soto *et al.*, 2010).

Based on seismic interpretations and commercial well data in the area close to mud-volcanoes in the northern area of the Diapiric Province (Perejil and Alhambra mud-volcanoes; Fig. 1), it has been concluded that the diapiric structures are rooted in the under-compacted shales from Unit VI and possibly the lower Unit V (Comas *et al.,* 1999; Talukder *et al.*, 2003).

Shale structures in the northern WAB form either isolated elliptical diapirs or elongated ridges (or walls) with two perpendicular trends: SW-NE and NNW-NNE (Fig. 1).

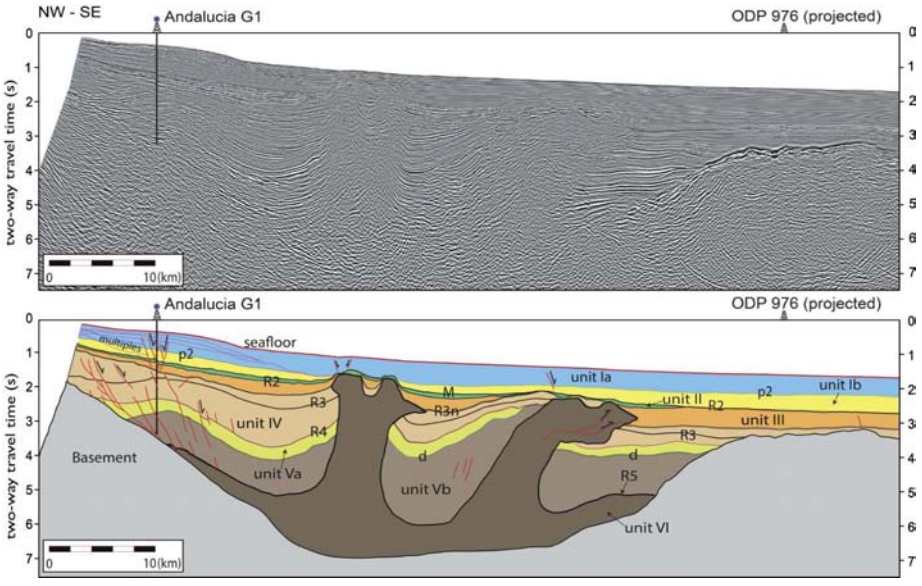

Fig. 2.- Seismic line (A) and interpretation (B) in the northern margin of the WAB. Seismic Units and discontinuities follow the seismo-stratigraphy of Comas *et al.* (1999). Position of the seismic line is shown in figure 1. See color figure in the web.

Fig. 2.- Perfil sísmico (A) e interpretación (B) en el margen norte de WAB. Las unidades y discontinuidades sísmicas siguen la sismo-estratigrafía de Comas* et al. *(1999). La posición de la línea sísmica se indica en la figura 1. Ver figura en color en la web.

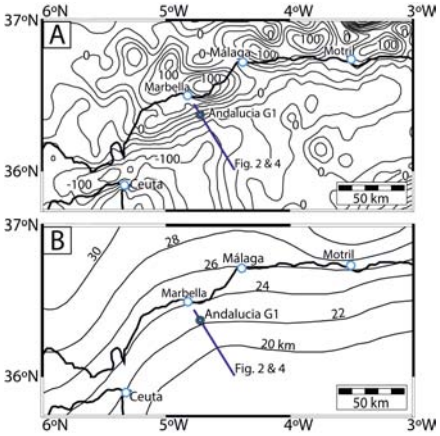

Fig. 3.- (A) Free Air anomaly contour map (contour intervals are 20 mGal) of the NW WAB (taken from Sandwell *et al.*, 2014). (B) Contour map of the Moho (contour intervals are 2 km) from Díaz and Gallart (2009). It is included the position of the modeled profile (Figs. 2 and 4).

Fig. 3.- (A) Mapa de contornos de la anomalía de la gravedad de Aire Libre (intervalos cada 20 mGal) del área estudiada (tomado de Sandwell* et al.*, 2014). (B) Mapa de contornos de profundidades de la Moho (intervalos cada 2 km) (Díaz y Gallart, 2009). Incluye la posición del perfil modelado (Figs. 2 y 4).

Seismic Interpretation

A regional seismic reflection profile running NW-SE in the northern margin of the WAB has been selected to model the gravity response of shale structures in this basin (Figs. 1 and 2). The studied seismic profile contains the Andalucía G1 well and shows two shale diapirs.

The interpretation shown in figure 2 illustrates the structural styles of the shale structures from the margin to the depocenter axis (Soto *et al.*, 2010; Fernández-Ibáñez and Soto, 2017). In this direction, marginal SE-dipping growth faults detached along the basement-cover (shale) detachment, shale anticlines, walls and a limited allochthonous shale-sheet are observed.

A syncline appears in the central area of the profile being flanked by two major diapiric forms.

Depth conversion

Time-depth conversion was done using the sonic velocities measured in the Andalucía G1 well (Fernández-Ibáñez and Soto, 2017). The average velocities for Unit VI were estimated in 2500 m/s, which is in agreement with V_p estimates in argillaceous sediments (*e.g.*, Mondol *et al.*, 2007). The average velocities for the other units are detailed in Table I.

2D Gravity modeling

A 2D gravimetric model was performed along the seismic profile, using Oasis Montaj software of Geosoft®. The interpretation of the section using gravity data involved two main stages: depth conversion and modeling of the formations. This interpretation refinement was achieved by comparing the synthetic gravity response of the different test models with the observed gravity.

Gravity data and crustal model

It has been used the Free Air gravity anomaly (track spacing ~285.5 m) taken from a regional dataset to model (extracted from the satellite model of Sandwell *et al.*, 2014). Figure 3A shows the regional Free Air gravity anomaly used for this study and the position of the modeled 2D section. It should be taken into account that the gravity dataset has a considerable spacing and it has a limited resolution to model small-scale structures.

The Moho depth along the modeled profile has been extracted from the compilation made by Díaz and Gallart (2009) (Fig. 3B).

Various average densities of the different sedimentary layers and checking the density and geometries of the basement-cover contact and the Moho has been tested using the Oasis Montaj software in an iterative process. The density values to obtain a better fit between the model and the observations is shown in Table I for the different units.

Gravity Model

The best gravity model obtained is shown in figure 4, with an average error of 4.97%. Seven different layers have been considered: water layer (1.04 g/cm^3), Pliocene and Pleistocene sediments (2.00 g/cm^3), non-diapiric Miocene sediments (2.30 g/cm^3), three sedimentary layers within the shale diapirs, divided according to depth (2.05, 2.15, and 2.35 g/cm^3), crustal basement (2.75-2.80 g/cm^3), and lithosphere mantle (3.20 g/cm^3).

There is a basinwards increase in the thickness of the Neogene to Quaternary sediments (Units V to I) to ~8 km, which is in agreement with previous estimates (Soto *et al.*, 2008). The thickness of the mobile shales (Unit VI; Lower Miocene) increases basinwards and the downslope shale migration seems to be blocked by the basement high at the SE of the section (corresponding to the Site 976 High).

Layers	V_p (m/s)	Density (g/cm^3)
sea water	1484	1.04
Plio-Pleistocene	2010	2.00
non-diapiric Miocene seds.	2800	2.30
upper shale	2500	2.05
middle shale	2500	2.15
lower shale	2500	2.35
crustal basement	n.a.	2.75-2.82
lithosphere mantle	n.a.	3.20

Table I.- Vp and densities used in this study. n.a.: not applicable.

Tabla I.- Vp y densidades usadas en este estudio. n.a.: no aplicable.

Shale diapirs are rooted in the lowermost sedimentary sequence (Un. VI). It has been confirmed the occurrence towards the SE of a partially-allochthonous shale sheet with a limited horizontal displacement (~5 km).

Although due to the nature of the modeled gravity data local anomalies above the shale diapirs are not identified, we inferred the occurrence of two diapirs with increasing densities with depth. Mobile shales ascent up to the Pliocene-Pleistocene boundary, at about 1 km depth, piercing in total 6-6.5 km of Miocene sediments, which results to be the total high of the shale diapirs. Maximum and minimum depths for the basement occur at ~8 km (in the depocenter axis) and between 2 and ~3 km in the NW margin and in the Site 976 basement high, respectively.

To model the shale diapirs, the best gravity model is obtained using three layers with average densities of 2.05, 2.15, and 2.35 g/cm^3. These values coincide with the density trend of clay-rich sediments formed by a clay fraction with approximately 60% of kaolinite and 40% of smectite (*e.g.*, Mondol *et al.*, 2007). This could be the clay-fraction composition for the overpressured shales of Unit VI, complementing the studies of the extruded sediments in the associated mud volcanoes (*e.g.*, Gennari *et al.*, 2013).

With respect to the basement, we inferred a variable density from the margin of the WAB

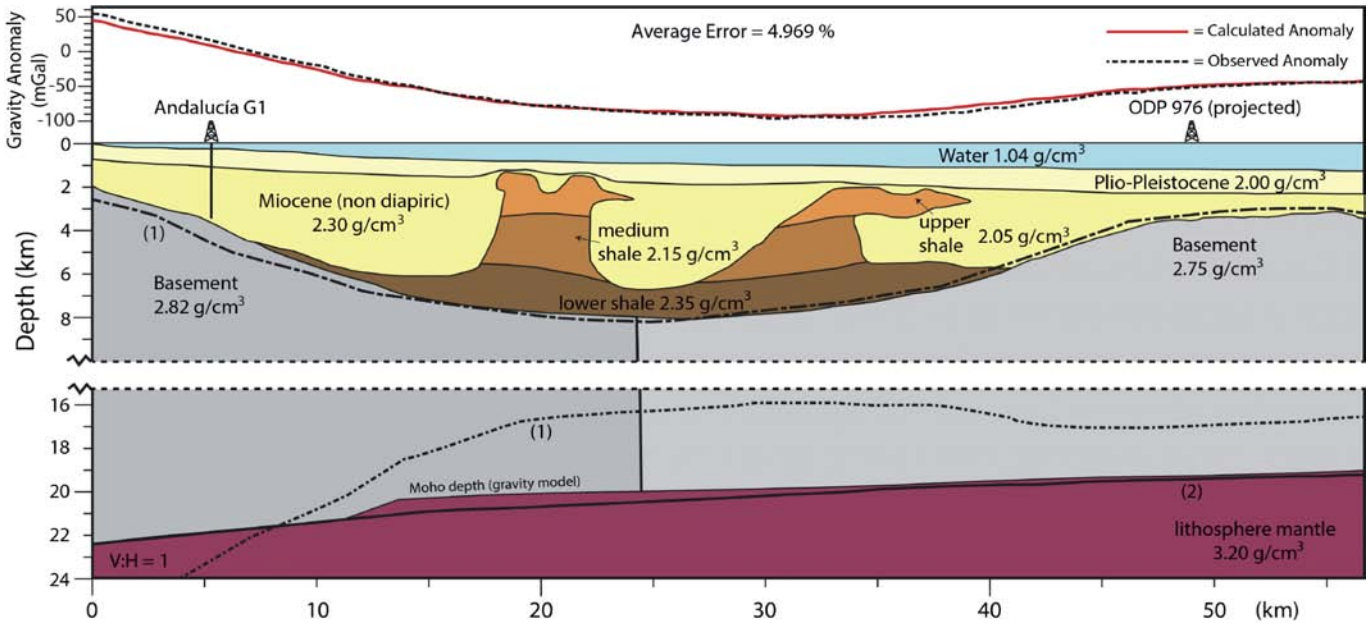

Fig. 4.- 2D gravity model detailing the different layers and their corresponding density (in g/cm3). Base of the sedimentary infill in the WAB together with the Moho depth are compared with data from Soto *et al.* (2008) (1) and Díaz and Gallart (2009) (2), respectively.See color figure in the web.

Fig. 4.- Modelo 2D gravimétrico con las distintos capas y sus correspondientes densidades (en g/cm3). La base del relleno sedimentario en la WAB y la profundidad de la Moho se comparan con datos de Soto* et al. *(2008) (1) y Díaz y Gallart (2009) (2), respectivamente. Ver figura en color en la web.

(2.82 g/cm^3) to the basement high of the Site 976 (2.75 g/cm^3). The first value corresponds to the average density value estimated by Soto *et al.* (2008) for the crust in the Betics and Rif. The crustal density reduction towards the SE is in agreement with the occurrence of crustal melts, like those sampled at ODP Site 976 (*e.g.*, Comas *et al*., 1999). The modeled Moho ascends from 22 km in the margin to about 19 km beneath the Site 976 basement high. It is inferred the occurrence of a sharp Moho step at about 12-13 km of horizontal distance. These values are similar to the geometry depicted by the model of Díaz and Gallart (2009), differing from the abrupt thinning inferred by authors like Soto *et al.* (2008).

Conclusions

(1) We have model a 2D gravity model coinciding with a seismic profile in the northern margin of the WAB. The seismic interpretation shows two major shale diapirs fed by overpressured shales from the lowermost sedimentary unit (Un. VI, Aquitanian-Burdigalian).

(2) A depth conversion of the interpreted profile has been accomplished to conduct the gravity modeling. The maximum sedimentary thickness of about 8 km is achieved between the two shale diapirs.

(3) The modeled gravity data has been extracted from a smoothed regional free air gravity anomaly from Sandwell *et al.* (2014). The best-fit model is formed by the layers: Plio-Pleistocene sediments (2.00 g/cm^3), Miocene sediments (2.30 g/cm^3), three slices of Lower Miocene shales divided according to depth (2.05, 2.15, and 2.35 g/cm^3, from top to bottom), crustal basement (2.75-2.82 g/cm^3), and lithosphere mantle (3.20 g/cm^3). The modeled Moho shallows basinwards, from 22 to 19 km.

(4) The inferred densities for the mobile shales (seismic Unit VI) agree with an average composition of the clay fraction formed by a mixture of kaolinite (60%) and smectite (40%).

Acknowledgements

This work was made possible thanks to the support of Repsol. We also acknowledge ConocoPhillips® for providing the seismic line which is the base of this study. IHS® for providing a Kingdom license and Geosoft® for an Oasis Montaj license through academic agreements with the Granada University. We are indebited to Antonio Azor and Antonio Olaiz for their comments, which have help to improve this paper. This contribution is part of the Research Group RNM-376.

References

Comas, M.C., Platt, J. P., Soto, J.I. and Watts, A.B. (1999). In: *Proceedings of the Ocean Drilling Program, Scientific Result*, 161, 555-580.

Díaz, J. and J. Gallart (2009). *Physics of the Earth and Planetary Interiors* 173, 181-190.

Férnández-Ibáñez, F. and Soto, J.I. (2017). *AAPG Bulletin* 101, 233-264.

Gennari, G., Spezzaferry, S., Comas, M.C., Rüggeberg, A., López-Rodríguez, C. and Pinheiro, L.M. (2013). *Marine Geology* 339, 83-95.

Jurado, M.J. and Comas, M.C. (1992). *GeoMarine Letters* 12, 129-136.

Mondol, N.H., Bjørlykke, K., Jahren, J., and Høeg, K. (2007). *Marine and Petroleum Geology* 24, 289-311.

Pérez-Belzuz, F., Alonso, B., and Ercilla, G. (1997). *Tectonophysics* 282, 399-422.

Sandwell, D.T., Müller R.D., Smith W.H., García, F.E., and Francis, R. (2014). *Science* 346, 65-67.

Sautkin, A., Talukder, A.R., Comas, M.C., Soto, J.I., and Alekseev, A. (2003). *Marine Geology* 195, 237-261.

Soto, J.I., Fernández-Ibáñez, F., Fernàndez., M., and García-Casco, A. (2008). *Geochemistry, Geophysics, Geosystems* 9, 1-27.

Soto, J.I., Fernández-Ibáñez, F., Talukder, A.R., and Martínez-García, P. (2010). In: *Shale Tectonics*. (L.J. Wood, Ed.) AAPG, 119-144.

Talukder, A.R., Comas, M.C., and Soto, J.I. (2003). *Geological Society, London, Special Publications* 216, 443-459.

Wood, L. J. (2012). In*: Regional Geology and Tectonics: Phanerozoic Passive Margins, Cratonic Basins and Global Tectonic Maps.* (D.G. Roberts and A.W. Bally, Eds.). Elsevier, 43-61.